ChemComm

COMMUNICATION

View Article Online
View Journal

Check for updates

Cite this: DOI: 10.1039/d6cc01163b

Received 24th February 2026,
Accepted 23rd April 2026

DOI: 10.1039/d6cc01163b

rsc.li/chemcomm

Supramolecular glass formation by arene–perfluoroarene pairing of three-dimensional macrocycles

Katsuto Onishi, [a] Shunsuke Ohtani, *[a] Kenichi Kato, [a] Shigehisa Akine [bc] and Tomoki Ogoshi *[ab]

We report supramolecular glass formation by mixing two crystalline pillar[6]arenes bearing benzyl and pentafluorobenzyl substituents, even though neither compound exhibited a melting point. The glass formation was attributed to arene–perfluoroarene interactions and the sterically bulky, three-dimensional pillar[6]arene framework that hinders efficient packing.

Molecular glasses, consisting of low-molecular-weight organic compounds, generally exhibit superior transparency, homogeneity, and isotropic properties compared with most polymer glasses.[1] Owing to these properties, they have attracted attention for applications such as organic light-emitting diodes and resist materials.[2]

The most common method for preparing glass materials is melting, followed by cooling. Melting effectively disrupts ordered molecular packing, which suppresses crystallization (Fig. 1a). Therefore, compounds that cannot be melted are fundamentally unsuitable for molecular glass formation.

Here, we discovered that mixing two crystalline pillar[6]arenes, one having benzyl groups (**B[6]**) and the other having pentafluorobenzyl groups (**PFB[6]**), neither of which exhibits a melting point, results in the formation of a molecular glass (Fig. 1b). The **B[6]** and **PFB[6]** ground powder mixture had a glass transition and was converted into a transparent film upon heating above and then cooling below the glass transition temperature (T_g). To the best of our knowledge, this is the first example of a molecular glass prepared from two crystalline, low-molecular-weight, organic molecules, neither of which has a melting point. We attributed the glass formation to two factors: the sterically bulky pillar[6]arene scaffold and intermolecular arene–perfluoroarene (AP) interactions between the benzyl and pentafluorobenzyl groups on the two components. Strong interactions between electron-rich aromatic and electron-deficient perfluoroaromatic groups[3] enhance miscibility, while the three-dimensional, distorted pillar[6]arenes[4] hinder efficient packing and thus suppress crystallization.

First, we synthesized two pillar[6]arene derivatives with benzyl groups **B[6]** and pentafluorobenzyl groups **PFB[6]** (Fig. 2a). Perethylated pillar[6]arene (**E[6]**) and unit models of **B[6]** and **PFB[6]** without macrocyclic structures (**B** and **PFB**) were also prepared as reference compounds (Fig. 2a). All new compounds were characterized with ^{1}H, ^{13}C and ^{19}F NMR spectroscopy and mass spectrometry (see supplementary information (SI)).

To obtain the structural information, single crystals of **B[6]** and **PFB[6]** were obtained (Fig. 2b, c, and Fig. S13). **B[6]** formed a highly symmetric pillar-shaped structure. In contrast, **PFB[6]** had a distorted conformation where orientations of the six units were not aligned. The **PFB[6]** distortion could be attributed to repulsive interactions among the electron-rich fluorine atoms in the pentafluorobenzyl groups.

Next, thermal properties of **B[6]** and **PFB[6]** were examined with thermogravimetry-differential thermal analysis (TG-DTA) and differential scanning calorimetry (DSC). The former indicated onsets of decomposition temperatures at approximately 250 °C and 200 °C for **B[6]** and **PFB[6]**, respectively (Fig. S14). In the DSC curves, there were no peaks until the decomposition temperatures of **B[6]** and **PFB[6]** (Fig. 2d). These results indicated that neither **B[6]** nor **PFB[6]** underwent a melting or a glass transition prior to the thermal decomposition. This could be attributed to the high molecular rigidity arising from the presence of multiple aromatic rings in both structures. In contrast, the 1 : 1 **B[6]**/**PFB[6]** ground mixture exhibited a T_g at 82 °C in the first cycle (Fig. 2d). The second cycle also exhibited the T_g at the same points during heating and cooling (Fig. S15). Hence, the ground mixture could be vitrified by heating above and then cooling below T_g.

Accordingly, we prepared a molecular glass by mixing **B[6]** and **PFB[6]** in the following steps: (i) Physically mixing **B[6]** and **PFB[6]** in a 1 : 1 molar ratio *via* grinding with an agate mortar,

[a] Department of Synthetic Chemistry and Biological Chemistry, Graduate School of Engineering, Kyoto University, Katsura, Nishikyo-ku, Kyoto 615-8510, Japan. E-mail: otani.shunsuke.6k@kyoto-u.ac.jp, ogoshi.tomoki.3s@kyoto-u.ac.jp
[b] WPI Nano Life Science Institute (WPI-NanoLSI), Kanazawa University, Kakuma-machi, Kanazawa, 920-1192, Japan
[c] Graduate School of Natural Science and Technology, Kanazawa University, Kakuma-machi, Kanazawa, 920-1192, Japan

Open Access Article. Published on 23 April 2026. Downloaded on 5/15/2026 9:04:04 AM. This article is licensed under a Creative Commons Attribution-NonCommercial 3.0 Unported Licence.

Open Access Article. Published on 23 April 2026. Downloaded on 5/15/2026 9:04:04 AM.
This article is licensed under a Creative Commons Attribution-NonCommercial 3.0 Unported Licence.

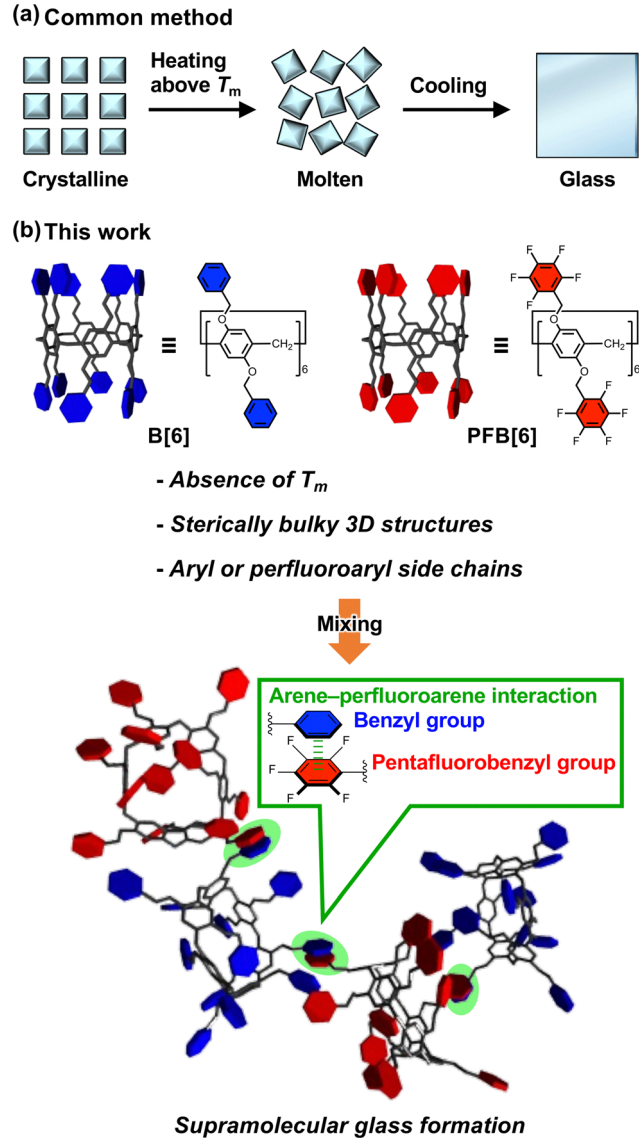

Fig. 1 Schematic representations of (a) common method for preparing glass materials and (b) formation of a molecular glass by mixing two pillar[6]arenes with benzyl groups (**B[6]**) and pentafluorobenzyl groups (**PFB[6]**) reported in this work.

(ii) heating the mixture at 100 °C for 10 min, and (iii) cooling to 25 °C (Fig. 2e). The powder mixture changed into a transparent viscous state upon heating in step (ii). After cooling in step (iii), the viscous state did not revert to the pristine powder, but instead formed a new transparent film (denoted as **B[6]$_1$–PFB[6]$_1$**, Fig. 2e). Powder X-ray diffraction (PXRD) analysis of **B[6]$_1$–PFB[6]$_1$** revealed only amorphous halos with no Bragg diffractions in contrast to the numerous sharp peaks of **B[6]** and **PFB[6]** (Fig. 2f). We also measured transmittance of **B[6]$_1$–PFB[6]$_1$** by the UV-vis spectroscopy, resulting in a transmittance of 80% (Fig. S16). These results clearly demonstrate the formation of a molecular glass by mixing two crystalline, low-molecular-weight, organic compounds that had no melting points.

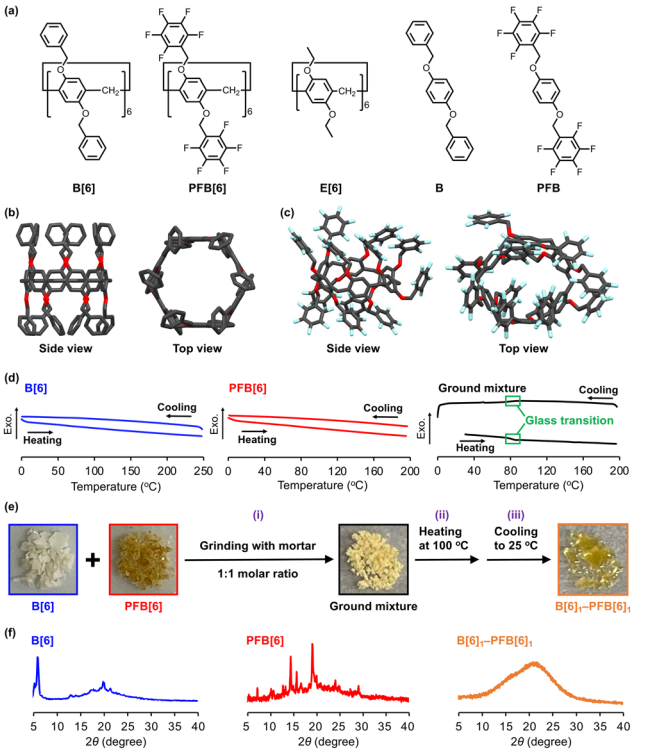

Fig. 2 (a) Chemical structures of **B[6]**, **PFB[6]**, **E[6]**, **B** and **PFB**. Single-crystal structures of (b) **B[6]** and (c) **PFB[6]**. In the structures, C: gray, O: red, F: light blue; all H atoms and cyclohexane molecules within the cavities of **B[6]** and **PFB[6]** are omitted for clarity. (d) DSC second heating and cooling curves of **B[6]** (left) and **PFB[6]** (middle), and first heating and cooling curves of the ground mixture of **B[6]** and **PFB[6]** (right). All scanning rates were 10 °C min^{-1}. (e) Procedure for preparation of **B[6]$_1$–PFB[6]$_1$**. (f) PXRD patterns of **B[6]** (left), **PFB[6]** (middle) and **B[6]$_1$–PFB[6]$_1$** (right).

The morphology of **B[6]$_1$–PFB[6]$_1$** was investigated *via* scanning electron microscopy (SEM). The images showed a smooth surface with no grain boundaries at the nanometre scale, in contrast to the significant gaps and grain boundary features in **B[6]** and **PFB[6]** images (Fig. 3a). SEM-energy dispersive X-ray (EDX) spectroscopy in elemental mappings of fluorine species indicated that **PFB[6]** was uniformly distributed throughout **B[6]$_1$–PFB[6]$_1$** (Fig. 3b). These results clearly demonstrated homogeneous mixing of **B[6]** and **PFB[6]** at the nanoscale (see Note S1 and Fig. S17 for the porosity of **B[6]$_1$–PFB[6]$_1$**).

We also prepared mixtures with other **B[6]:PFB[6]** molar ratios (**B[6]$_1$–PFB[6]$_2$** and **B[6]$_2$–PFB[6]$_1$**) using the same procedure as for the 1:1 sample **B[6]$_1$–PFB[6]$_1$**. In contrast to **B[6]$_1$–PFB[6]$_1$**, both **B[6]$_1$–PFB[6]$_2$** and **B[6]$_2$–PFB[6]$_1$** were

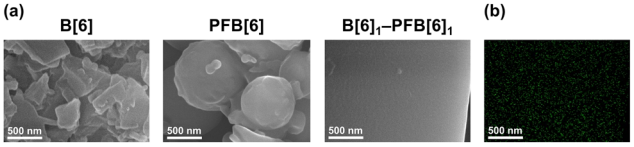

Fig. 3 (a) SEM images of **B[6]**, **PFB[6]** and **B[6]$_1$–PFB[6]$_1$**. (b) SEM-EDX elemental mapping of fluorine species on **B[6]$_1$–PFB[6]$_1$**.

This journal is © The Royal Society of Chemistry 2026

Open Access Article. Published on 23 April 2026. Downloaded on 5/15/2026 9:04:04 AM.
This article is licensed under a Creative Commons Attribution-NonCommercial 3.0 Unported Licence.

opaque solids (Fig. S18). PXRD peaks in **B[6]**$_1$–**PFB[6]**$_2$ were similar to those for **PFB[6]** (Fig. S19). Similarly, the **B[6]**$_2$–**PFB[6]**$_1$ peaks closely resembled those of **B[6]** (Fig. S20). These results indicated that **B[6]**$_1$–**PFB[6]**$_2$ and **B[6]**$_2$–**PFB[6]**$_1$ contained crystalline domains derived predominantly from the higher-ratio components in each mixture, suggesting that only the 1 : 1 molar ratio yielded a uniform glass material.

To identify the factors governing formation of the **B[6]**$_1$–**PFB[6]**$_1$ glass state, we performed control experiments on various pairs of **B[6]**, **PFB[6]** and reference compounds **E[6]**, **B** and **PFB** (Fig. 2a). Mixing was conducted *via* the three-step procedure described above.[5a] The resulting samples were denoted as **B**$_1$–**PFB**$_1$, **B[6]**$_1$–**PFB**$_6$, **PFB[6]**$_1$–**B**$_6$, **B[6]**$_1$–**E[6]**$_1$, and **PFB[6]**$_1$–**E[6]**$_1$. For **B[6]**$_1$–**PFB**$_6$ and **PFB[6]**$_1$–**B**$_6$, six molar equivalents of **PFB** and **B** were added per macrocycle.[5b]

B$_1$–**PFB**$_1$ was a powder and showed different diffraction peaks from those of the **B** and **PFB** constituents (Fig. S21), indicating that it was a co-crystal instead of a molecular glass. This suggested that AP interactions attributed to the relatively planar **B** and **PFB** structures. Similarly, the opaque **B[6]**$_1$–**PFB**$_6$ and **PFB[6]**$_1$–**B**$_6$ solids exhibited many sharp PXRD peaks (Fig. S22). These results demonstrated that three-dimensional scaffolds of pillar[6]arenes in the **B[6]** and **PFB[6]** constituents were important in preventing formation of crystalline assemblies. **B[6]**$_1$–**E[6]**$_1$ and **PFB[6]**$_1$–**E[6]**$_1$ were also powders, and their PXRD patterns were superposed on the those of the constituents **B[6]** and **E[6]**, and **PFB[6]** and **E[6]** (Fig. S23). These results indicated that both benzyl and pentafluorobenzyl groups, as well as the sterically bulky pillar[6]arene skeleton, were necessary for molecular glass formation.

In our previous study, the introduction of fluoroalkyl groups into pillar[*n*]arene scaffolds enabled glass formation through a melt-cooling process.[6] In contrast, this work demonstrates a distinct mechanism for supramolecular glass formation *via* mixing of two crystalline components, neither of which exhibits a melting transition (see Note S2 and Fig. S24 and S25 for information about pillar[5]arene derivatives).

To verify AP interactions in **B[6]**$_1$–**PFB[6]**$_1$, we acquired Fourier transform infrared (FT-IR) spectra for **B[6]**, **PFB[6]** and **B[6]**$_1$–**PFB[6]**$_1$ (Fig. 4a). **B[6]** bands at 694 cm^{-1} and 733 cm^{-1}, attributable to C–H out-of-plane bending of monosubstituted benzene rings, shifted to 699 cm^{-1} and 737 cm^{-1} in **B[6]**$_1$–**PFB[6]**$_1$, respectively (Fig. 4b). Additionally, the C–F stretching band of the pentafluorobenzyl groups in **PFB[6]** shifted from 976 cm^{-1} to 979 cm^{-1} in **B[6]**$_1$–**PFB[6]**$_1$ (Fig. 4c). These shifts indicated that benzyl groups in **B[6]** and pentafluorobenzyl groups in **PFB[6]** participated in AP interactions upon glass formation.

Furthermore, TG curve for **B[6]**$_1$–**PFB[6]**$_1$ exhibited only one degradation step, with the decomposition onset temperature at approximately 230 °C, which was between those of **B[6]** and **PFB[6]** (Fig. S26 and S27). This suggested that **B[6]**$_1$–**PFB[6]**$_1$ uniformly decomposed as a consequence of the intimate mixing. Interestingly, over 40% of the **B[6]**$_1$–**PFB[6]**$_1$ weight remained even after heating to 900 °C, in contrast to the absence of residual mass for **B[6]** and **PFB[6]**, indicating strong

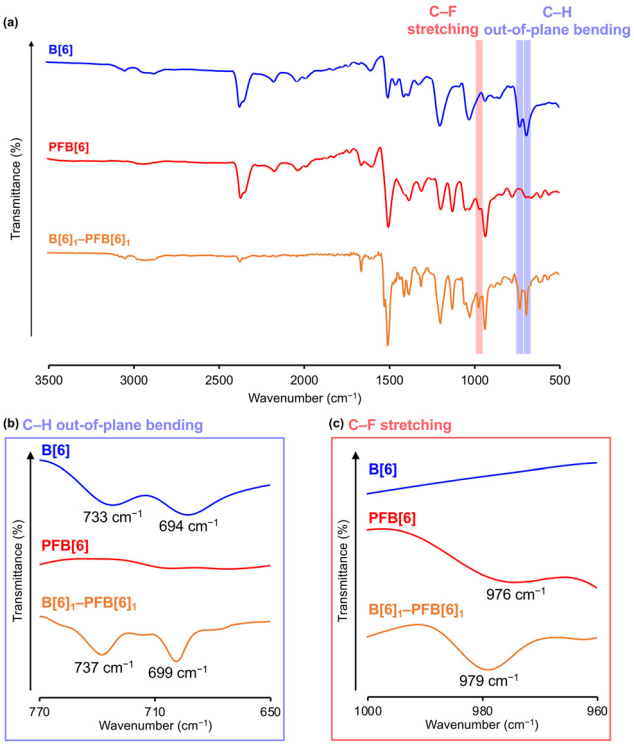

Fig. 4 (a) FT-IR spectra of **B[6]**, **PFB[6]** and **B[6]**$_1$–**PFB[6]**$_1$. Enlarged views of (a) in the (b) C–H out-of-plane bending and (c) C–F stretching regions.

AP interactions between **B[6]** and **PFB[6]** in **B[6]**$_1$–**PFB[6]**$_1$. Taken together, the FT-IR and TGA results both verified that AP interactions were formed and that the equimolar glass was both compositionally homogeneous and thermally robust.

In general, amorphous mixtures remain stable against crystallization (devitrification) when maintained approximately 50 K below their T_g. This is because the mobilities of the component molecules are greatly reduced.[7] In this context, the stability of **B[6]**$_1$–**PFB[6]**$_1$, which exhibited a T_g at 82 °C, was examined at room temperature. The appearances, PXRD patterns and transmittances did not change even after 6 months in air (Fig. S28), indicating that the glass state of **B[6]**$_1$–**PFB[6]**$_1$ was stable at room temperature for at least half a year.

Previous studies have reported that assemblies composed of arene and perfluoroarene exhibit room-temperature phosphorescence (RTP) because of accelerated intersystem crossing with enhanced spin–orbit coupling *via* AP interactions.[8] However, the effect has been predominantly observed in crystalline materials. Motivated by these studies, we examined the optical properties of glassy **B[6]**$_1$–**PFB[6]**$_1$. Kubelka–Munk transformed diffuse reflectance (DR) spectrum of **B[6]**$_1$–**PFB[6]**$_1$ revealed a broad absorption band with a maximum at 344 nm (Fig. S29). Upon excitation at 344 nm at room temperature, **B[6]**$_1$–**PFB[6]**$_1$ gave a single phosphorescence band at 562 nm with a lifetime of 70 ms (Fig. 5a, b and see Note S3 and Fig. S30, S31 for further phosphorescence measurements under controlled atmosphere and variable temperature conditions). In contrast, there were no peaks in the spectra for **B[6]** or **PFB[6]** (Fig. S32). Although

Open Access Article. Published on 23 April 2026. Downloaded on 5/15/2026 9:04:04 AM.
This article is licensed under a Creative Commons Attribution-NonCommercial 3.0 Unported Licence.

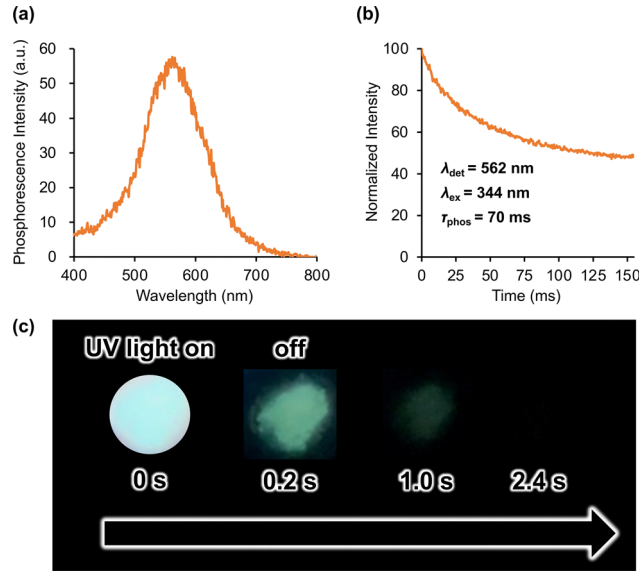

Fig. 5 (a) Steady-state phosphorescence spectrum of **B[6]$_1$–PFB[6]$_1$** (λ_{ex} = 344 nm). (b) RTP lifetime decay curve for **B[6]$_1$–PFB[6]$_1$**. Both spectra in (a) and (b) were acquired at room temperature in air. (c) Luminescence photographs of **B[6]$_1$–PFB[6]$_1$** under 340 nm UV light irradiation and at different times after the irradiation. All photographs in (c) were acquired at room temperature in air immediately after cooling to 77 K.

the RTP of **B[6]$_1$–PFB[6]$_1$** was too weak to be visible at room temperature, yellow-green emission was confirmed upon cooling to 77 K (Fig. 5c). The co-crystal of unit models **B$_1$–PFB$_1$** also emitted RTP at 559 nm with a lifetime of 82 ms (Fig. S33). Therefore, AP interactions were essential for RTP emission in this system. RTP-active molecular glasses are rare,[9] and, to the best of our knowledge, this is the first example of exploiting AP interactions to form a molecular glass that exhibits RTP.

In conclusion, we have successfully prepared a molecular glass by mixing two types of pillar[6]arene derivatives: one bearing benzyl groups and the other bearing pentafluorobenzyl groups. Remarkably, even though neither crystalline constituent exhibited a distinct T_m, the glass readily formed *via* simple physical mixing, followed by mild thermal treatment. Comprehensive investigations revealed that the glass formation was driven by two key factors: the sterically bulky architecture of the pillar[6]arene skeleton and intermolecular AP interactions.

The AP interactions enabled RTP, which is rare in molecular glasses. Because of their high optical transparency, suppression of self-quenching and light scattering and excellent processability into thin films and coatings, this molecular glass is a promising RTP emitter. Overall, our findings provide new design principles for molecular glasses and highlight their potential as materials for practical applications.

Tomoki Ogoshi and Shunsuke Ohtani conceptualized and supervised the work., Katsuto Onishi and Shigehisa Akine designed and performed experiments. The first draft of the manuscript was written by Katsuto Onishi, Shunsuke Ohtani, and Tomoki Ogoshi. All authors analyzed and discussed the results, and co-wrote the paper.

Conflicts of interest

There are no conflicts to declare.

Data availability

Data supporting this article have been included in the supplementary information (SI). Supplementary information is available. See DOI: https://doi.org/10.1039/d6cc01163b.

CCDC 2531301 and 2531501 contain the supplementary crystallographic data for this paper.[10a,b]

Acknowledgements

This work was supported by JST CREST Grant Number JPMJCR24S6 (T. O.), Japan, JSPS KAKENHI Grant Numbers JP25K18086 (Early-Career Scientists, S. O.), JP22K19063 (Challenging Research (Exploratory), T. O.), JP25H00896 (Scientific Research (A), T. O.), JP24K21247 (Challenging Research (Pioneering), T. O.), JST SPRING, Grant Number JPMJSP2110 (K. O.), JSPS Research Fellowship for Young Scientists: JP25KJ1616 (K. O.), and the MEXT World Premier International Research Center Initiative (WPI), Japan. Dr Takeshi Yamamoto and Prof. Dr Michinori Suginome (Kyoto University) for PXRD measurement. We thank Edanz (https://jp.edanz.com/ac) for editing a draft of this manuscript.

References

1 (*a*) Y. Shirota, *J. Mater. Chem.*, 2000, **10**, 1–25; (*b*) Y. Shirota, *J. Mater. Chem.*, 2005, **15**, 75–93.
2 (*a*) L.-H. Chan, R.-Ho Lee, C.-F. Hsieh, H.-C. Yeh and C.-T. Chen, *J. Am. Chem. Soc.*, 2002, **124**, 6469–6479; (*b*) A. D. Silva, N. M. Felix and C. K. Ober, *Adv. Mater.*, 2008, **20**, 3355–3361; (*c*) J. Chen, Q. Hao, S. Wang, S. Li, T. Yu, Y. Zeng, J. Zhao, S. Yang, Y. Wu, C. Xue, G. Yang and Y. Li, *Acs. Appl. Polym. Mater.*, 2019, **1**, 526–534; (*d*) D. Umeyama, S. Horike, M. Inukai, T. Itakura and S. Kitagawa, *J. Am. Chem. Soc.*, 2015, **137**, 864–870; (*e*) T. D. Bennett and S. Horike, *Nat. Rev. Mater.*, 2018, **3**, 431–440; (*f*) N. Ma, H. Ando, R. Ma and T. Nakanishi, *Small*, 2026, e14459; (*g*) X. Jiang, X. Cui, A. J. E. Duncan, L. Li, R. P. Hughes, R. J. Staples, E. V. Alexandrov, D. M. Proserpio, Y. Wu and C. Ke, *J. Am. Chem. Soc.*, 2019, **141**, 10915–10923.
3 (*a*) O. R. Lozman, R. J. Bushby and J. G. Vinter, *J. Chem. Soc., Perkin Trans.*, 2001, **2**, 1446–1452; (*b*) S. Lorenzo, G. R. Lewis and I. Dance, *New J. Chem.*, 2000, **24**, 295–304; (*c*) J. Hernández-Trujillo, F. Colmenares, G. Cuevas and M. Costas, *Chem. Phys. Lett.*, 1997, **265**, 503–507; (*d*) A. P. West, Jr., S. Mecozzi and D. A. Dougherty, *J. Phys. Org. Chem.*, 1997, **10**, 347–350; (*e*) Z. Huang, X. Chen, G. Wu, P. Metrangolo, D. Whitaker, J. A. McCune and O. A. Scherman, *J. Am. Chem. Soc.*, 2020, **142**, 7356–7361; (*f*) H. Zhang, J. Han, X. Jin and P. Duan, *Angew. Chem., Int. Ed.*, 2021, **60**, 4575–4580; (*g*) W. Wu, C. Ye, J. Qin and Z. Li, *ACS Appl. Mater. Interfaces*, 2013, **5**, 7033–7041; (*h*) X. Ji, H. Wang, H. Wang, T. Zhao, Z. A. Page, N. M. Khashab and J. L. Sessler, *Angew. Chem., Int. Ed.*, 2020, **59**, 23402–23412.
4 (*a*) T. Ogoshi, T. Yamagishi and Y. Nakamoto, *Chem. Rev.*, 2016, **116**, 7937–8002; (*b*) K. Jie, Y. Zhou, E. Li, Z. Li, R. Zhao and F. Huang, *J. Am. Chem. Soc.*, 2017, **139**, 15320–15323; (*c*) T. Ogoshi, K. Saito, R. Sueto, R. Kojima, Y. Hamada, S. Akine, A. M. P. Moeljadi, H. Hirao, T. Kakuta and T. Yamagishi, *Angew. Chem., Int. Ed.*, 2018, **57**, 1592–1595; (*d*) K. Jie, M. Liu, Y. Zhou, M. A. Little, A. Pulido, S. Y. Chong, A. Stephenson, A. R. Hughes, F. Sakakibara, T. Ogoshi, F. Blanc, G. M. Day, F. Huang and A. I. Cooper, *J. Am. Chem. Soc.*, 2018, **140**, 6921–6930; (*e*) K. Jie, Y. Zhou, E. Li and F. Huang, *Acc. Chem. Res.*, 2018, **51**, 2064–2072; (*f*) K. Jie, Y. Zhou, E. Li,

Open Access Article. Published on 23 April 2026. Downloaded on 5/15/2026 9:04:04 AM.
This article is licensed under a Creative Commons Attribution-NonCommercial 3.0 Unported Licence.

R. Zhao and F. Huang, *Angew. Chem., Int. Ed.*, 2018, **57**, 12845–12849.

5 (*a*) The heating temperatures in the step (ii) were set between the melting points and the thermal decomposition temperatures of the components; (*b*) In the preparation of mixtures of **B[6]** and **PFB**, and **PFB[6]** and **B**, the number of moles of benzyl and pentafluorobenzyl groups were equalized to provide proper comparisons with $\mathbf{B[6]}_1$–$\mathbf{PFB[6]}_1$. To this end, the corresponding pillar[6]arenes and unit models were mixed in a 1 : 6 molar ratio in both cases.

6 K. Onishi, S. Ohtani, K. Kato, S. Fa, Y. Sakata, S. Akine, M. Ogasawara, H. Asakawa, S. Nagano, Y. Takashima, M. Mizuno and T. Ogoshi, *Chem. Sci.*, 2022, **13**, 4082–4087.

7 (*a*) L. Yu, *Adv. Drug Delivery Rev.*, 2001, **48**, 27–42; (*b*) S. V. Bhujbal, B. Mitra, U. Jain, Y. Gong, A. Agrawal, S. Karki, L. S. Taylor, S. Kumar and Q. T. Zhou, *Acta Pharm. Sin. B*, 2021, **11**, 2505–2536.

8 (*a*) Q. Zhang, Y. Fan, Q. Liao, C. Zhong, Q. Li and Z. Li, *Sci. China: Chem.*, 2022, **65**, 918–925; (*b*) X. Pang, H. Wang, W. Wang and W. J. Jin, *Cryst. Growth Des.*, 2015, **15**, 4938–4945; (*c*) Q. Liao, Q. Li and Z. Li, *Adv. Mater.*, 2025, **37**, 2306617.

9 (*a*) J. J. Flynn, Z. M. Marsh, D. M. Krein, S. M. Wolf, J. E. Haley, E. S. Vasquez, T. M. Cooper, N. P. Godman and T. A. Grusenmeyer, *ChemPhotoChem*, 2022, **6**, e202200134; (*b*) M. Zhang, X. Lan, M. Ding, C. Han, X. W. Liu, Z. Meng, Z.-Q. Yu and Z. An, *Angew. Chem., Int. Ed.*, 2025, **64**, e202415250.

10 (*a*) CCDC 2531301: Experimental Crystal Structure Determination, 2026, DOI: 10.5517/ccdc.csd.cc2qz0wm; (*b*) CCDC 2531501: Experimental Crystal Structure Determination, 2026, DOI: 10.5517/ccdc.csd.cc2qz7b9.